Novel biosensing device for point-of-care applications with plastic antibodies grown on Au-screen printed electrodes

Felismina T.C. Moreira , Rosa A.F. Dutra , João P.C. Noronha , João C.S. Fernandes , M. Goreti F. Sales

ABSTRACT

A gold screen printed electrode (Au-SPE) was modified by merging Molecular Imprinting and Self- Assembly Monolayer techniques for fast screening cardiac biomarkers in point-of-care (POC). For this purpose, Myoglobin (Myo) was selected as target analyte and its plastic antibody imprinted over a glutaraldehyde (Glu)/cysteamine (Cys) layer on the gold-surface. The imprinting effect was produced by growing a reticulated polymer of acrylamide (AAM) and N,N'-methylenebisacrylamide (NNMBA) around the Myo template, covalently attached to the biosensing surface. Electrochemical impedance spectroscopy (EIS) and cyclic voltammetry (CV) studies were carried out in all chemical modification steps to confirm the surface changes in the Au-SPE.

The analytical features of the resulting biosensor were studied by different electrochemical techniques, including EIS, square wave voltammetry (SWV) and potentiometry. The limits of detection ranged from
0.13 to 8 µg/mL. Only potentiometry assays showed limits of detection including the cut-off Myo levels. Quantitative information was also produced for Myo concentrations ≥ 0.2 µg/mL. The linear response of the biosensing device showed an anionic slope of ~ 70 mV *per* decade molar concentration up to 0.3 µg/mL.The interference of coexisting species was tested and good selectivity was observed. The biosensor was
successfully applied to biological fluids.

1. Introduction

Acute myocardial infarction (AMI) leads to myocardium necrosis and to an increasing number of specific biomolecules flowing in the blood and being excrete through urine, such as Myo [1]. Myo is the first biomolecule increasing after AMI [2–4], offering a high sensitive way to detect or exclude AMI conditions within 1–5 h of symptom onset [1]. Subsequent Myoglobinuria is also observed within 4–50 h [4].

Any intended protocol to determine Myo in POC must produce low turnaround times to detect such rapid biochemical alterations and be sufficiently cheap to be used routinely. Analytical data must be produced for normal/abnormal Myo ranges without requiring complex sample pre-treating steps. Myo cut-off levels range from 100–200 ng/mL [5–7]. The higher levels of Myo vary a

lot, with previous studies showing 420–2000 ng/mL in serum [8] and 450 ng/mL in urine [9].

Several methods based on enzymatic and immunoassay was described in the literature [10]. The first methods for Myo determination in blood were all supported by immunoreactions, including radioimmunoassay [8,11,12], counterimmunoelectrophoresis [13] enzyme-immunoassay [8] chemiluminescent immunoassay [14] and latex agglutination immunoassay [15–17], later coupled to turbidimetric [18] or nephelometric [19,20] readings and to other solid support materials, such as polystyrene [20]. In subsequent years many attempts have been made to create suitable devices for POC applications [21,22]. They employ various transducer principles but keep the immunochemical background. Immunoassays have the main advantage of offering a selectivity/specificity that cannot be matched by the chemical methods, but they lack the stability and the low price of these.

A successful route to replace the immunoassays is the synthesis of plastic antibodies [23–25]. These materials are prepared by growing a solid polymer structure around a target compound, creating sites that are expected to be complementary in size and electrostatic environment to the imprinted molecule. These sites

may rebind the analyte, in a similar way to that of natural antibodies. This concept has been proven successful for designing many biosensing devices [26], including Myo [24]. This work describes the surface imprinting of Myo on silica beads and its inclusion in PVC membranes. Myo was detected successfully, but not as low as cut-off levels. A previous work on surface imprinting may also be found, but no analytical data on the performance of the device is given.

The design of Myo plastic antibodies is however a challenging task [27]. Protein imprinting offers several critical aspects, due to its complex structure and variable spatial arrangement. A successful plastic antibody design should meet the exact conditions under which the native protein exists. The use of many biocompatible monomeric materials, such as acrylamide and bisacrylamide that can be polymerized in aqueous environments, is a classical way to achieve such conditions [28]. On the other hand, considering that surface imprinting is a bottom-up approach, resembling nature's processes of building complex structures, this should be the logical strategy for designing plastic antibodies for proteins.

Two special requirements are needed for a successful plastic antibody based device for Myo determination in POC: (i) it should be disposable to allow a direct and easy handling [28] of biological fluids in hospitals; and (ii) it should allow the covalent link of the plastic antibody to the biosensing surface, in order to ensure that it remains there after its contact with a liquid phase. The first requirement may be achieved by using SPE technology. The huge developments of this field originated a massive production of inexpensive, reproducible and sensitive disposable electrodes. The second requirement may be fulfilled by selecting gold surfaces. Over the past decades [29], many biosensors have used self-assembled monolayers (SAMs) as a way to immobilize, in an ordered manner, organic molecules on gold surfaces [30]. This organic thin-film material layer may turn out a successful and highly controlled way to link the imprinting layer to the gold surface.

Therefore, the main goal of this work is to develop a biosensing device with plastic antibodies imprinted on Au-SPE modified by self-assembly for POC applications. The resulting biosensor is evaluated by several electrochemical techniques and further applied to the analysis of biological samples.

2. **Experimental**

2.1. *Apparatus*

The electrochemical measurements were conducted in a potentiostat/galvanostat from Metrohm Autolab/PGSTAT302 N, with a FRA2 module and controlled by ANOVA 7.0 software. Au-SPEs were purchased from DROPSENS (DRP-C220AT), having working and counter electrodes made of gold and reference electrode and electrical contacts made of silver. The diameter of the working electrode was 4 mm.

For electrochemical assays the SPEs were place in a switch box from DROPSENS, interfacing the electrical contacts of the Au-SPE with the electrical connections of the potentiostat/galvanostat. In Potentiometry assays a Crison, GLP 21 pH meter (± 0.1 mV sensitivity) was used with an Ag wire covered by a layer of AgCl acting as reference electrode. Readings were made at room temperature and under constant stirring.

2.2. *Reagents*

All chemicals were of analytical grade and de-ionized water (conductivity <0.1 μS/cm) was employed. Potassium hexacyanoferrate III, potassium hexacyanoferrate II-3-hydrate and

sodium hydrogenophosphate dihydrate were obtained from Riedel Haen; potassium chloride, (hydroxymethyl)aminomethane (Tris) and potassium di-hydrogenphosphaste from Panreac; 2-(N-morpholino)ethanesulfonic acid monohydrate 98% (MES), from Alfa Aesar; sodium chloride, glutaraldehyde 25% (Glu), 2-aminoethanethiol 95% (Cys), hydrogen peroxide 30%, ethanol 99.5%, Myo, AAM, NNMBA, ammonium persulphate (APS), oxalic acid (Oac), and sodium chloride from Fluka. Creatinine (Creat), hemoglobin (Hmg), Bovine Serum albumin (BSA), sodium glutamate (Glt) and urea were tested as interfering species and obtained from Fluka.

2.3. *Solutions*

Stock solutions of 5.0×10^{-6} mol/L Myo were prepared in MES buffer (1.0×10^{-3} mol/L, pH 4.5). Less concentrated standards were prepared by accurate dilution of the previous solution in buffer.

Electrochemical assays were performed with 5.0×10^{-3} mol/L $K_3[Fe(CN)_6]$ and $K_4[Fe(CN)_6]$ in MES 1.0×10^{-3} mol/L, pH 7. The selectivity study used 1.0×10^{-6} mol/L Myo solutions prepared buffer. Solutions of interfering species were of variable concentrations and prepared in the same buffer. Creat (5.25×10^{-5} mol/L), Hmg (5.0×10^{-6} mol/L), BSA (5.1×10^{-6} mol/L), Glt (7.61×10^{-5} mol/L) and urea (5.4×10^{-5} mol/L) solutions were prepared for this purpose.

2.4. *Design of the plastic antibody on the Au-SPE*

The gold surface of the working electrode was incubated in 25 mmol/L ethanolic solutions of Cys for 4 h, at 25 °C. The resulting Cys/Au-SPE was washed with distilled water and incubated for 50 min in Glu 2.5%, prepared in 0.1 mol/L PBS, pH 7.0, at 4 °C. The Glu/Cys/Au-SPE was washed with PBS and kept in 1×10^{-6} mol/L Myo prepared in PBS buffer, pH 7.0, for 4 h, at 4 °C. The electrode was thoroughly washed again with PBS buffer to remove adsorbed Myo. The Myo/Glu/Cys/Au-SPE was then incubated in 0.5 mol/L Tris for 30 min. and thoroughly washed with deionized water. The imprinting stage started by adding 10 μL of 1.0 mol/L AAM and 0.07 mol/L NNMBA, prepared in PBS, pH 7.0, to the modified gold. This was followed by the addition of 10 μL of 0.06 mol/L APS solution in PBS pH 7.0. The polymerization was carried out at 25 °C, for 4 h. The sensor was thoroughly washed with deionized water and incubated in diluted Oac for 12 h. Oac is able to break peptide bonds, allowing a successful removal of the protein from the imprinted layer [27].

The imprinted sensor was washed and conditioned in 10 mmol/L PBS buffer, pH 7.4.

2.5. *AFM analysis*

The morphological analysis of the MIP material, before and after protein removal, and the negative control NIP was conducted by atomic force microscopy (AFM) in tapping mode. This was done in a Veeco Metrology Multimode/Nanoscope IVA. Nanoscope software was used to analyse the AFM images.

2.6. *Electrochemical assays*

CV and SWV measurements were conducted in 5.0 mmol/L of $[Fe(CN)_6]^{3-}$ and 5.0 mmol/L of $[Fe(CN)_6]^{4-}$, prepared in MES buffer, pH 7.0. For CV assays the potential was scanned from -0.5 to +0.7 V, at 30 mV/s. In SWV studies potentials were changed from -0.4 to +0.7 V, at a 0.125 V/s, corresponding to a frequency of 20 Hz and step height of 150 mV.

EIS assays were conducted with the same redox couple $[Fe(CN)_6]^{3-/4-}$ at a standard potential of 0.225 V, using a sinusoidal potential perturbation with amplitude 0.01 V (RMS) and a number
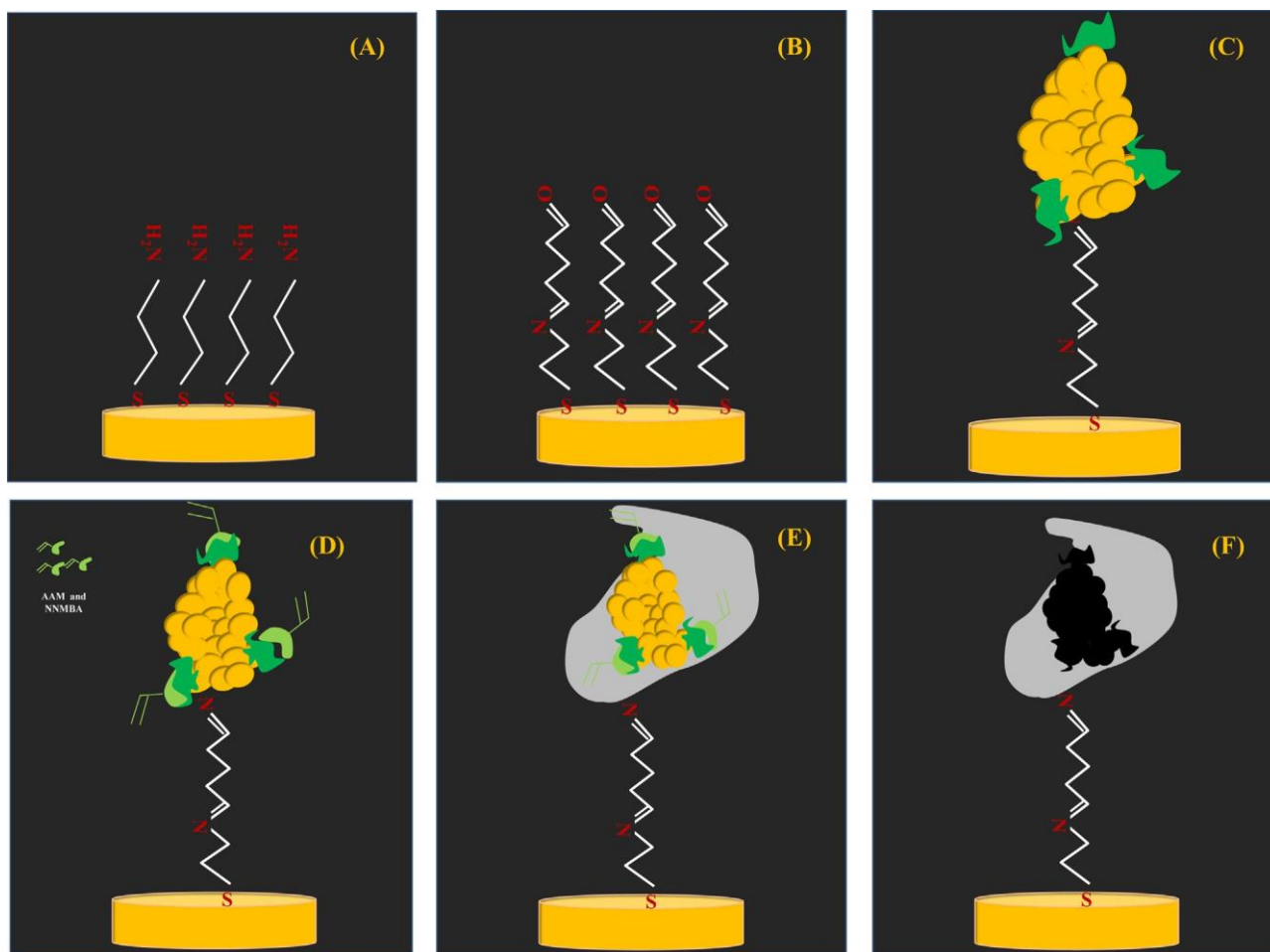
Fig. 1. Assembly of the Au-SPE imprinted device.

of frequencies equal to 50, logarithmically distributed over a frequency range of 0.1–100 kHz. The impedance data were fitted to a Randles equivalent circuit using the implemented ANOVA software.

Potentiometric measurements were made at room temperature and under constant stirring, after stabilization to ± 0.2 mV. Increasing concentrations of Myo were obtained by transferring 0.0100 to 0.200 mL aliquots of 7.2×10^{-6} mol/L Myo aqueous solution to a 10 mL beaker containing 5.00 mL of 1.0×10^{-3} mol/L of MES, of fixed pH and ionic strength. Between assays, the sensors were conditioned in 1.0×10^{-5} mol/L Myo solution.

2.7. Selectivity

Potentiometric selectivity coefficients were calculated by the Matched Potential Method (MPM), using Eq. (1). The initial concentration of primary ion was set to 2.0×10^{-7} mol/L (a_A) and an aliquot of a primary ion solution of 5.0×10^{-6} mol/L, changing the concentration $a_{A'}$, was added, increasing the potential in ~ 16 mV. The interference of Crea, Hmg, BSA, Glt, and Urea was assessed by adding small aliquots (a_B) of the corresponding solutions (Section 2.3) into the primary ion solution (of a_A), until the same potential change was observed, i.e., until an increment of ~ 16 mV was reached, ensuring that the final concentration of primary ion was not altered by more than 5%.

Potentiometric analysis by single standard addition (SAM).

$$K_{A,B}^{POT} = \frac{(a_{A'} - a_A)}{a_B} \tag{1}$$

2.8. Urine samples analysis

The single standard addition method, Eq. (2), was used, where c_0 and V_0 are the unknown analyte concentration and the initial volume of the analyte sample, respectively [31]; c and V are the concentration of the standard reference solution and the volume of its addition; and E_0 and E are the electrode potentials before and after adding the reference solution. The V_0 and c values were 5.0 mL and 5×10^{-6} mol/L respectively.

$$c_0 = \frac{c(V_2 - V_1)}{V_0(10^{(E_2 - E_0/S)} - 10^{(E_1 - E_2)/S})} \tag{2}$$

Results and discussion

3.1. Design of the biosensor

The working electrode of the Au-SPE was modified by following the scheme in Fig. 1. It consisted of six different stages, starting in (A) the formation of an amine layer, (B) made reactive in order to (C) bind the protein. The imprinting step was started by (D) self-organizing the monomeric structures around the template and (E) polymerizing with cross-linker and initiator. The imprinted sites were obtained (F) once the protein was removed.

The amine layer (Fig. 1A) was formed by incubating the gold surface in Cys. Its contact with a gold substrate leads to the spontaneous formation of a closely packed monolayer via a strong gold-sulfur interaction between the SH groups and the gold. This

monolayer has a standing-up configuration with the amine groups (–NH$_2$) exposed to the surrounding environment.

The external layer of primary amines was modified by reaction with Glu (Fig. 1B). Glu carries two terminal aldehyde functions (–CHO) to which amines react under mild conditions by means of a nucleophilic addition mechanism. The typical product is an imine (–C=N–), ensuring a covalent attach of Glu to the amine layer. Of course, the existence of two aldehyde functions in the same reactant (Glu) suggest great care in the selection of time, temperature, pH and concentration of Glu. One unaltered aldehyde function is expected to remain as an outer layer (Fig. 1B) and any deviation from the intended course leads to the reduction of the number of active carbonyls for subsequent binding of Myo. In the present work, the reaction took place with a diluted solution of Glu, at 4 °C, for 50 min. The pH was kept in 7.0, adjusting the surface conditions of the biosensor to receive a protein.

This new aldehyde layer is ready to react with Myo (Fig. 1C). Myo is a single polypeptide chain of 153 amino acids carrying all kinds of amino acid residues. It has a globular and compact nature (45 × 35 × 25 Å), with both polar and nonpolar amino acid side-chains directed to the external surface of the protein. The exact amount and nature of these residues are however difficult to identify because proteins are not rigid objects as their biological function is controlled by conformational changes of different magnitudes [32]. Therefore, it is reasonable to assume the existence of some external function in Myo that will be able to react with the previous aldehyde layer. Any aliphatic amine or alcohol will be able to carry out this reaction. Of course the pH of this assay must be equal to that in physiological conditions, ensuring the same degree of protonation in each side-chain. The aldehyde functions that remained unaffected after binding Myo were blocked with Tris to prevent unexpected reactions.

The imprinting stage started by incubating the Au-SPE with Myo in AAM allowing their self-organization around the protein (Fig. 1D). NNMBA was added after, along with the initiator, producing a radical polymerization (Fig. 1E). The time and monomer/cross-linker concentrations given in this stage were of particular importance because if the polymer layer turns out too thick it may entrap the protein irreversibly. The temperature at which this polymerization reaction took place was also important because the imprinted conformation should match that of Myo in the samples. Ambient temperature was selected in this stage considering that the sample analysis is also carried under this temperature condition. Finally, the attached protein was after removed later by reaction with Oac [27] to empty the imprinted sites (Fig. 1F). Subsequently, several washing steps were performed to remove the released peptide fractions from the sensory surface.

3.2. Control of the surface modification

The immobilization of organic films on metal surfaces produces global modifications in the electrical features of the solid-state probe. This can be measured by monitoring the changes in the electron transfer capability of well-known redox systems, such as [Fe(CN)$_6$]$^{4-}$/[Fe(CN)$_6$]$^{3-}$. Indirect ways of measuring such alterations include EIS and CV [33].

EIS studies were used to follow the Au-SPE modification after each chemical change. Randle's equivalent circuit was adopted to model the physiochemical process occurring at the gold electrode surface (Fig. 2A), as it is often used to interpret simple electrochemical systems [34]. The elements of this circuit include the uncompensated resistance of the solution phase (R_S), the capacitance of the double layer (C_{dl}), and charge-transfer resistance (R_{ct}) which is inversely proportional to the rate of electron transfer, and the Warburg diffusion element (W), accounting for the diffusion of ions from bulk electrolyte to the electrode interface.

The EIS spectra of this Randle's equivalent circuit were recorded for every step of the Au-SPE surface modification and the results were presented as Nyquist plots (Fig. 2A). The typical plots may include a semicircle region lying on the real axis followed by a straight line. The semicircle was observed at high frequency range and indicated a charge-transfer controlled process. The diameter of this semicircle equaled the R_{ct} controlling the electron transfer kinetics of the redox-probe at the electrode interface [35]. The linear range was given at the low frequency range and showed diffusion-controlled process from mass-transfer.

The bare gold electrode showed a very small semicircle domain, suggesting a very fast electron-transfer process with a diffusional limiting step (Fig. 2A). The consecutive attachments of the Cys and Glu gave rise to subsequent increases in the electron transfer resistance, resulting in increases in the semicircular section of the Nyquist plot. The linkage of Myo followed by the polymerization reaction produced an additional barrier for the redox probe access to the Au-SPE modified electrode. This resulted in an extra increase in the electron transfer resistance, reflected by further substantial increase in R_{ct}.

CV assays are shown in Fig. 2B and supported the previous studies of EIS. When compared to the redox probe in the bare gold, the subsequent modification steps of the Au-SPE increased the peak-to-peak potential separation in the voltammograms, accounting for the increased charge-transfer resistance. The cathodic peak decreased with additional modification steps and the anodic peak tended to disappear, attributing a similar-to-irreversible character to the reaction of the redox probe. This irreversibility was curiously reversed after the polymerization step, although the anodic and cathodic peak currents were much lower than that of the redox probe on the bare gold.

3.3. AFM analysis

The morphological analysis of the MIP before (A) and after (B) protein removal and the negative control NIP (C) was performed by AFM measurement (Fig. 3). Morphological differences were observed between all materials. The MIP material before removing the protein (A) in smother than the MIP material after oxalic acid treatment (B), evidencing the exit of the protein for the polymeric layer. Thus, the rugosity B may be attributed to the vacant places created by the protein removal (and not to polymeric changes from the oxalic acid treatment because the NIP surface does not a similar aspect). Furthermore, the "cavities" observed in this roughness ranged ~10 nm, suggesting that Myo was imprinted in monomeric or dimeric states (a single Myo molecule is 4.5 nm × 3.5 nm × 2.5 nm) [36].

3.4. Selection of the transducer

Many biosensors in POC employ electrochemical detection as transducer element because of the low cost, ease of use, portability, and simplicity of construction [37,38]. The monitored event changes a specific electrical property of the electrochemical cell, involving, in many cases, a measurable current over a potential range scanning (voltammetry), a measurable charge accumulation or potential at near-zero current (potentiometry), or a measurable resistive and capacitive properties upon perturbation of a system by a small amplitude sinusoidal AC excitation (impedance spectroscopy). These were the technical approaches taken in the present study.

The calibration of the modified Au-SPE in EIS assays checked the effect of Myo on the charge-transfer resistance of a redox probe. Comparing to the spectrum of the redox probe alone, Nyquist plots showed that diameter of the semicircles decreased gradually with increasing concentration of Myo. So, Myo reduced the
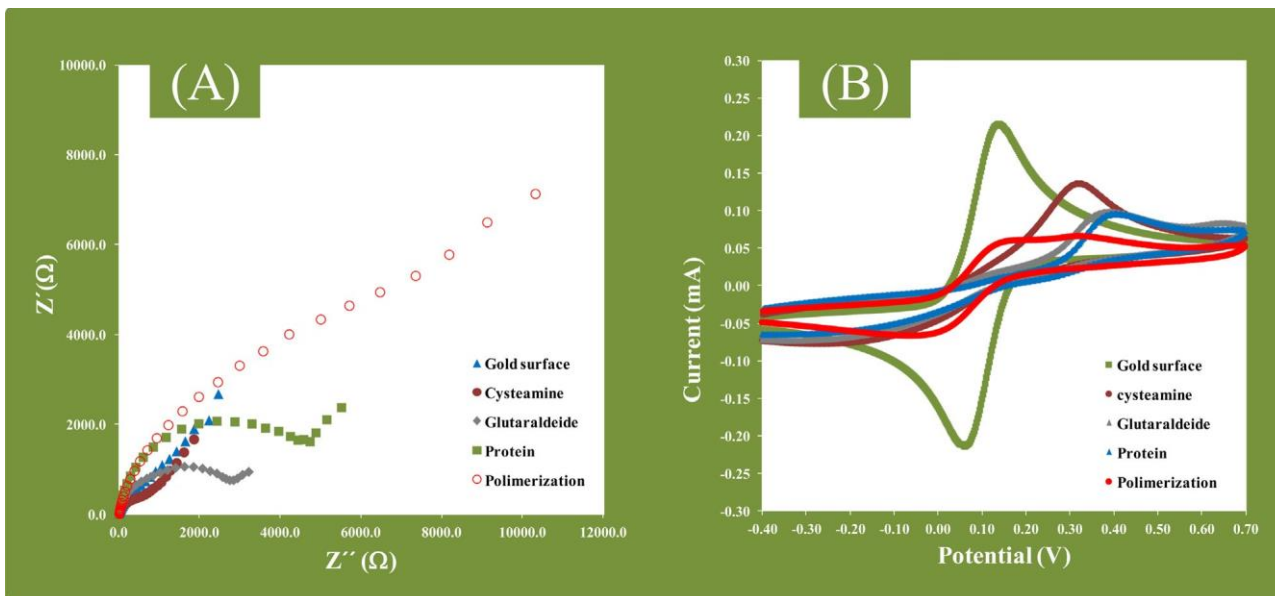
Fig. 2. Electrochemical controls of the subsequent modification steps of the Au-SPE in 5.0 mM $[Fe(CN)_6]^{3-}$ and 5.0 mM $[Fe(CN)_6]^{4-}$, in MES buffer pH 7, carried out by of EIS (A, Nyquist plot) and CV (B, cyclic voltammograms) assays.

charge-transfer resistance of the probe once bound to the imprinted sensory layer (Fig. 4A). This effect was checked for a concentration range of Myo varying from 0.16 to 48.6 μg/mL. Plots of $\log(R_{ct})$ against log[Myo] showed linear behavior from 9.0 to 36.0 μg/mL, with a limit of detection of 2.25 μg/mL (see Fig. 4B).

SWV was selected among other voltammetric methods for displaying high sensitivity to surface-confined electrode reactions, with suitable detection capabilities and rapidity. In general, the presence of Myo in the redox probe decreased its typical cathodic

peak current observed without Myo by the imprinted modified Au-SPE (Fig. 5A). In terms of overall analytical performance, it was possible to observe that this effect of Myo was consistent for all concentrations tested, ranging from 0.16 to 48.6 μg/mL. The electrochemical response resulted in a negative slope calibration (Fig. 5B) showing a linear behavior from 9.0 to 36 μg/mL of Myo. The limit of detection was 8.5 μg/mL.

Potentiometric measurements were conducted by calibrating the cell with Myo concentrations ranging from 0.10 to 46 μg/mL.
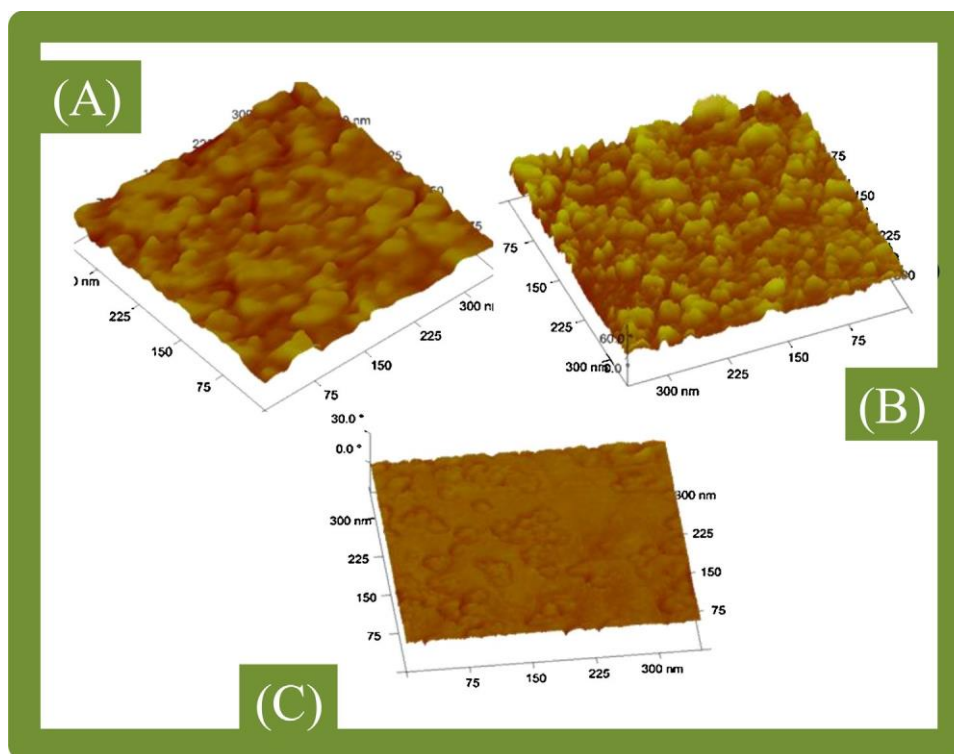
Fig. 3. AFM images of: (A) MIP material before protein removal; (B) MIP material after protein removal; and (C) NIP material. AFM images obtained in tapping mode, 300 × 300 nm scan, and processed using Nanorule program to show the 3-D topography.
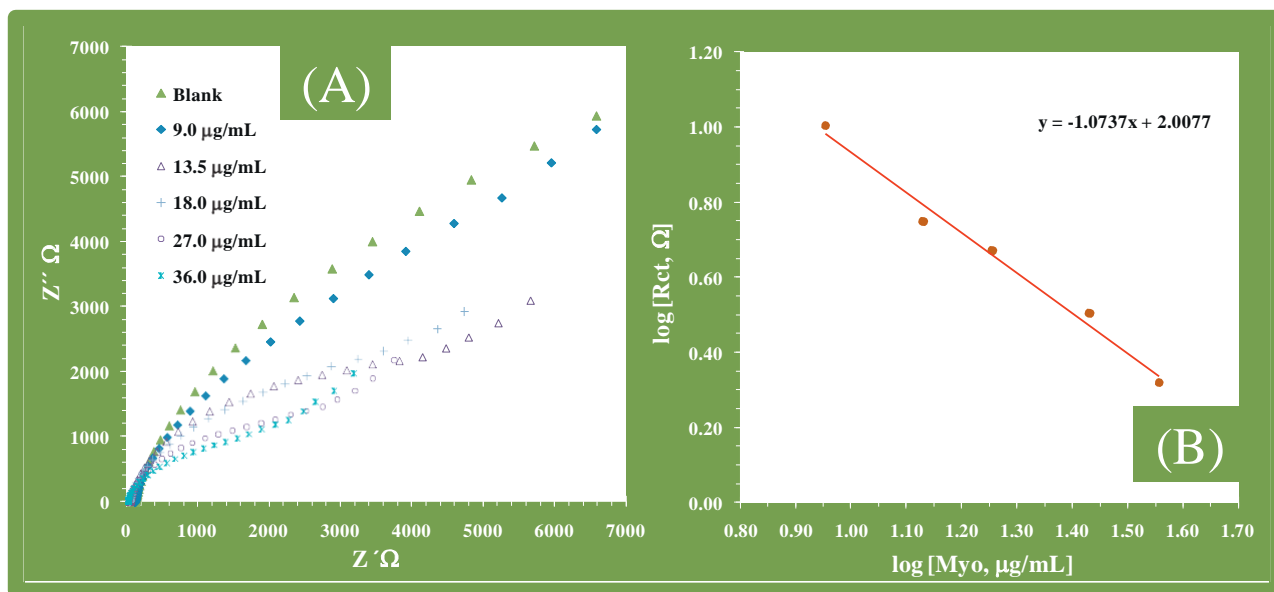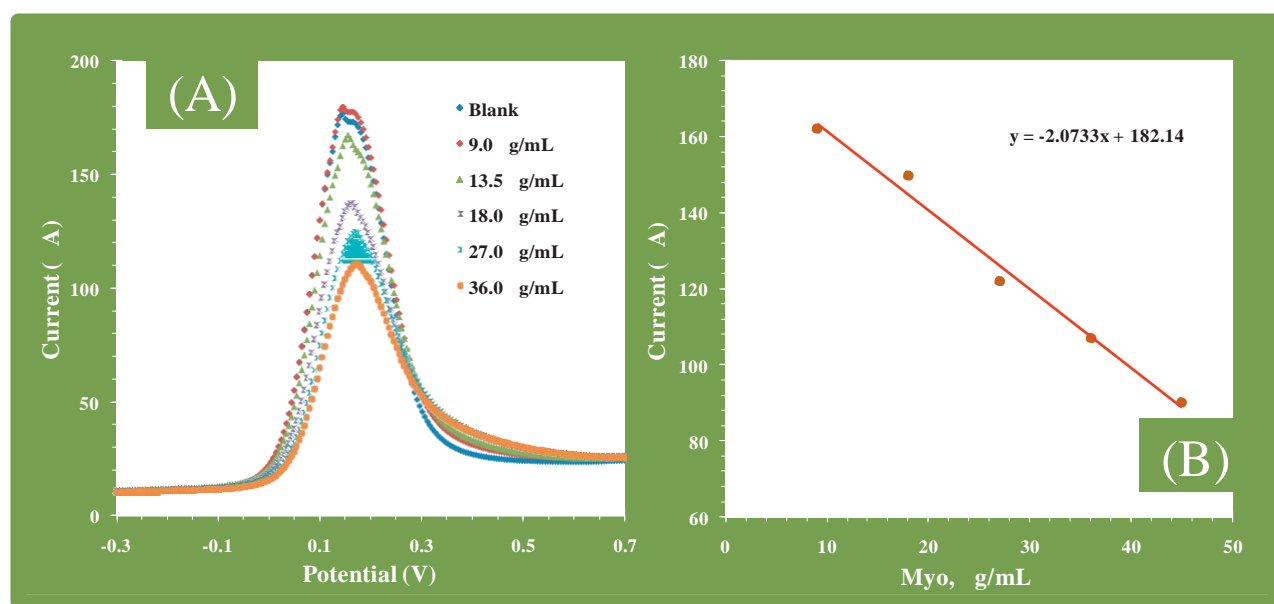
Fig. 4. EIS Nyquist plot (A) of modified Au-SPE and the corresponding calibration curve (B) in 5.0 mM [Fe(CN)$_6$]$^{3-}$ and 5.0 mM [Fe(CN)$_6$]$^{4-}$, in MES buffer pH 7, with different concentrations of Myo.

Tests carried out in a pH of 7.4 were unable to produce enough potential changes against concentration, and other pH conditions were tested. In general, the presence of Myo in pH 4.5 increased the potential change against concentration by decreasing the cell potential (Fig. 6). This behavior is typically attributed to negatively charged species, which was not as expected: Myo will be neutral in solutions matching its isoelectric point (7.2), positive in solutions of lower pH, and negative in solutions of higher pH. So, in a solution of pH 4.5 the net charge of Myo is positive. However, it is important to consider the protein great dimensions and its polyionic nature, carrying many positive and negatively-charged side chains. These conditions may imply non-equilibrium ion-exchange processes between the protein in the aqueous phase and sensory imprinted material in the solid-state electrode that may cause a large potential change, resulting in

a non-equilibrium super-Nernstian response. This would be consistent with the anionic slopes of -70.3 mV/decade. Furthermore, the use of ammonium persulphate as initiator may attribute the sensory surface positive charges, repealing the negative charged sites of the protein and attracting the positively charged ones. The linear behavior was observed within 0.348 and 24 μg/mL, with detection limit of 0.13 μg/mL. The squared correlation coefficients were always >0.992. The device also offered quick responses, with each standard requiring <30 s to reach a potential stability of ± 1 mV.

Overall, the widest linear range and the lower limit of detection were obtained for the potentiometric assays (Table 1). In terms of POC applications for Myo analysis in biological fluids, this approach was the only one reaching cut-off levels. Thus, potentiometric transduction was selected as transducer in subsequent

Fig. 5. SWV (A) of modified Au-SPE and the corresponding calibration curve (B) in 5.0 mM [Fe(CN)$_6$]$^{3-}$ and 5.0 mM [Fe(CN)$_6$]$^{4-}$, in MES buffer pH 7, with different concentrations of Myo.
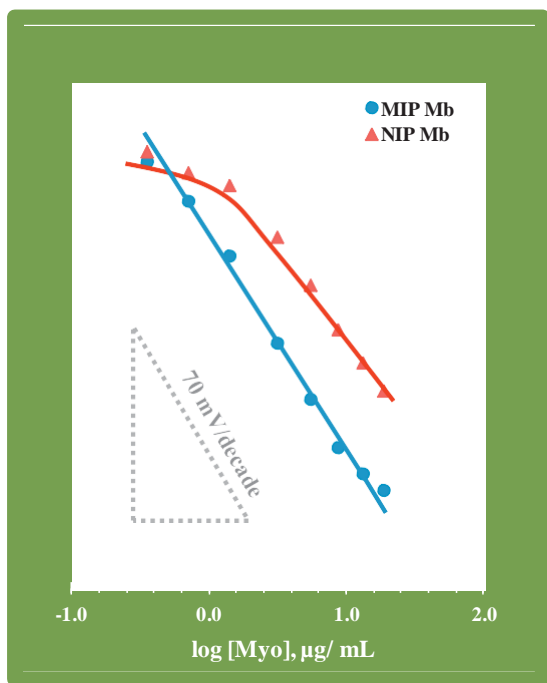
Fig. 6. Potentiometric calibration curves of MIP and NIP Au-SPE in MES buffer pH 7.

studies, including its selectivity against other biological species and its behavior under practical application.

The MIP biosensor was reused 3 times after several washes with buffer, and was stable for at least 3 weeks in solution.

3.5. Selectivity study

The selectivity of a membrane electrode is of major importance for a successful analytical application. It is governed mostly by the equilibrium that exists at the membrane-solution interface, and can be determined experimentally by calculating potentiometric selectivity coefficients, K^{POT}. These coefficients define the ability of an electrode to differentiate a primary ion from species that interfere in the analytical reading [39]. The lower the K^{POT} the smaller the interference.

The matched potential method (MPM) was selected in this study, because it does not require that the biosensors exhibit Nernstian behavior for the primary ion and interfering ions, nor that the ions are of equal charge (thus avoiding the difficulties in accuracy coming from the conventional methods) [39,40]. Furthermore it is valid and applicable to virtually any sensor as long as only small signal changes are considered [40].

The interfering species tested were selected among those that may be found in biological fluids, such as Crea, Hmg, BSA, Glt, and Urea. From these, only Hmg was able to promote a potential

variation of 15.8 mV. The required concentration was about 333 mg/L, corresponding to a potentiometric selectivity coefficient of -0.77. For Crea, Glt, BSA, and Urea, the corresponding potential changes were only 10.3; 5.4; 0.3 and 4.8 mV, respectively. The corresponding concentrations were 5.84, 332, 10.2 and 3.23 mg/L, all below the reference levels for the intended samples. Overall, the selectivity study confirmed the high selectivity of the potentiometric device, suggesting its possible application under real samples.

The stereo-selectivity of the imprinted Au-SPE was also tested by checking the response of Myo in a non-imprinted device, fabricated by using only PBS buffer in the step C of protein binding (Fig. 1). As may be seen in Fig. 5, the non-imprinted devices showed higher concentrations for linear ranges and detection limits with similar slope. Thus, the imprinting effect was observed only in the concentrations nearing the limit of detection. After that, Myo concentration starts being too high, leading to non-specific interactions at the membrane-solution interface. This may turn out especially relevant for Myo concentrations nearing cut-off levels

3.6. Myo assay

The standard addition method was applied to determine Myo in spiked urine samples, ranging from 0.48 to 0.96 μg/mL Myo. A good agreement was found between added and found amounts of Myo, with recoveries ranging 92.0 to 96.2%. Average relative standard deviations were 0.6%. These results pointed out the accuracy and the precision of the analytical data, suggesting that it may turn out a successful approach for screening AMI episodes in POC.

4. Conclusions

Surface imprinting of Myo was successfully established by merging self-assembled monolayer and molecular imprinting technologies on a single Au-SPE device and applying it to Myo detection/determination in biological fluids. Potentiometric transduction offered the best analytical features compared to EIS and SWV, suitable selectivity features for practical application and quick responses.

Overall, the potentiometric method with the imprinted Au-SPE device is simple, of low cost, precise, accurate and inexpensive, and may turn out in a near future an alternative method for screening Myo in POC.

Table 1

Main analytical features obtained with the different electrochemical transducers.

Analytical feature	Electrochemical impedance spectroscopy	Square-wave voltammetry	Potentiometry
Slope	-1.07^a	-2.08^b	-74.9^c
r^2	>0.987	>0.992	>0.992
LOD (μg/mL)	2.25	8.5	0.133
Lower linear range (μg/mL)	9.0	9.0	0.348
Response time (s)	<90	<30	<15

[a] $\log kQ/([Myo]/\mu g/mL)$.
[b] $uA/([Myo]/\mu g/mL)$.
[c] $mV/\log([Myo]/\mu g/mL)$.

References

[1] C.W. Hamm, Acute coronary syndromes – the diagnostic role of troponins, Thrombosis Research 103 (2001) S63–S69.

[2] J. Lim, R.C. Hawkins, K. Ng, S.P. Chan, A. Cheng, K.S. Ng, A preliminary study of the utility of combined cardiac markers in the evaluation of patients presenting early with suspected acute coronary syndrome, Annals Academy of Medicine Singapore 31 (6) (2002) 772–776.

[3] S. Galli, M. Villa, P. Montorsi, P. Ravagnani, F. Fabbiocchi, D. Trabattoni, A. Lualdi, C. Rossetti, G. Teruzzi, L. Grancini, et al., Impact of new post-procedural myocardial infarction definition in 3900 consecutive patients after PCI. Acute and 3 years clinical outcome, American Journal of Cardiology 104 (6A) (2009) 206D–207D.

[4] T.G. Donald, M.J. Cloonan, C. Neale, D.E.L. Wilcken, Excretion of myoglobin in urine after acute myocardial-infarction, British Heart Journal 39 (1) (1977) 29–34.

[5] E.G. Matveeva, Z. Gryczynski, J.R. Lakowicz, Myoglobin immunoassay based on metal particle-enhanced fluorescence, Journal of Immunological Methods 302 (1-2) (2005) 26–35.

[6] A.M. Castaldo, P. Ercolini, F. Forino, A. Basevi, L. Vrenna, P. Castaldo, V.D. Ambrosio, A. Castaldo, Plasma myoglobin in the early diagnosis of acute

myocardial-infarction, European Journal of Clinical Chemistry and Clinical Biochemistry 32 (5) (1994) 349–353.

[7] J. Woo, F.L. Lacbawan, R. Sunheimer, D. Lefever, J.B. McCabe, Is myoglobin useful in the diagnosis of acute myocardial-infarction in the emergency department setting, American Journal of Clinical Pathology 103 (6) (1995) 725–729.

[8] M.J. Stone, M.R. Waterman, D. Harimoto, G. Murray, N. Willson, M.R. Platt, G. Blomqvist, J.T. Willerson, Serum myoglobin level as diagnostic test in patients with acute myocardial-infarction, British Heart Journal 39 (4) (1977) 375–380.

[9] M.J. Cloonan, G.A. Bishop, P.D. Wiltonsmith, I.W. Carter, R.M. Allan, D.E.L. Wilcken, Enzyme-immunoassay for myoglobin in human-serum and urine – method development, normal values and application to acute myocardial-infarction, Pathology 11 (4) (1979) 689–699.

[10] A. Qureshi, Y. Gurbuz, J.H. Niazi, Biosensors for cardiac biomarkers detection: a review, Sensors and Actuators B: Chemical 171 (2012) 62–76.

[11] M.J. Stone, J.T. Willerson, M.R. Waterman, Radioimmunoassay of myoglobin in human-serum – results in patients with acute myocardial-infarction, Journal of Clinical Investigation 56 (5) (1975) 1334–1339.

[12] G. Gilkeson, M.J. Stone, M. Waterman, R. Ting, C.E. Gomezsanchez, A. Hull, J.T. Willerson, Detection of myoglobin by radioimmunoassay in human sera – its usefulness and limitations as an emergency room screening-test for acute myocardial-infarction, American Heart Journal 95 (1) (1978) 70–77.

[13] K. Hiramori, T. Sumiyoshi, S. Motegi, T. Honda, S. Kimata, K. Hirosawa, H. Kawai, A. Kondo, M. Iwaasa, K. Miyoshi, Rapid, sensitive detection of myoglobinemia by improved counterimmunoelectrophoresis in cases of acute myocardial-infarction, American Heart Journal 96 (2) (1978) 187–190.

[14] Y. Nishida, H. Kawai, H. Nishino, A sensitive sandwich enzyme-immunoassay for human myoglobin using Fab-horseradish peroxidase conjugate – methods and results in normal subjects and patients with various diseases, Clinica Chimica Acta 153 (2) (1985) 93–104.

[15] M.G. Bachem, K. Paschen, B. Strobel, H.E. Keller, B. Kleinschnittger, Myoglobin latex test – a rapid test for early diagnosis of acute myocardial-infarction, Deutsche Medizinische Wochenschrift 108 (31-3) (1983) 1190–1194.

[16] K. Norregaardhansen, J. Hangaard, B. Norgaardpedersen, A rapid latex agglutination-test for detection of elevated levels of myoglobin in serum and its value in the early diagnosis of acute myocardial-infarction, Scandinavian Journal of Clinical & Laboratory Investigation 44 (2) (1984) 99–103.

[17] J.P. Chapelle, C. Heusghem, Semi-quantitative estimation of serum myoglobin by a rapid latex agglutination method – an emergency screening-test for acute myocardial-infarction, Clinica Chimica Acta 145 (2) (1985) 143–150.

[18] E. Metzmann, B. Schmidt, M. Dengler, W. Kapmeyer, Quantitative myoglobin determination with a turbidimetric latex test, Journal of Clinical Chemistry and Clinical Biochemistry 26 (11) (1988), 760-760.

[19] A. Burlina, R. Bertorelle, D. Faggian, M. Zaninotto, M. Mussap, M. Plebani, Latex nephelometric immunoassay for the quantitative-determination of myoglobin in human serum, Clinical Chemistry 36 (6) (1990), 994-994.

[20] H.S. Lee, S.J. Cross, P. Garthwaite, A. Dickie, I. Ross, S. Walton, K. Jennings, Comparison of the value of novel rapid measurement of myoglobin, creatine-kinase, and creatine kinase-MB with the electrocardiogram for the diagnosis of acute myocardial-infarction, British Heart Journal 71 (4) (1994) 311–315.

[21] M.P. Hudson, R.H. Christenson, L.K. Newby, A.L. Kaplan, E.M. Ohman, Cardiac markers: point of care testing, Clinica Zanimica Acta 284 (2) (1999) 223–237.

[22] A.L. Straface, J.H. Myers, H.J. Kirchick, K.E. Blick, A rapid point-of-care cardiac marker testing strategy facilitates the rapid diagnosis and management of chest pain patients in the emergency department, American Journal of Clinical Pathology 129 (5) (2008) 788–795.

[23] H-Y. Lin, C-Y. Hsu, J.L. Thomas, S-E. Wang, H-C. Chen, T-C. Chou, The microcontact imprinting of proteins: the effect of cross-linking monomers for lysozyme, ribonuclease A and myoglobin, Biosensors & Bioelectronics 22 (4) (2006) 534–543.

[24] F.T.C. Moreira, R.A.F. Dutra, J.P.C. Noronha, M.G.F. Sales, Myoglobin-biomimetic electroactive materials made by surface molecular imprinting on silica beads and their use as ionophores in polymeric membranes for potentiometric transduction, Biosensors & Bioelectronics 26 (12) (2011) 4760–4766.

[25] R. Schirhagl, U. Latif, D. Podlipna, H. Blumenstock, Dickert F.L. Natural, Biomimetic materials for the detection of insulin, Analytical Chemistry 84 (9) (2012) 3908–3913.

[26] S.A. Piletsky, N.W. Turner, P. Laitenberger, Molecularly imprinted polymers in clinical diagnostics – future potential and existing problems, Medical Engineering & Physics 28 (10) (2006) 971–977.

[27] F. Bonini, S. Piletsky, A.P.F. Turner, A. Speghini, A. Bossi, Surface imprinted beads for the recognition of human serum albumin, Biosensors & Bioelectronics 22 (9–10) (2007) 2322–2328.

[28] H.L. Zhao, T.Y. Guo, Y.Q. Xia, M.D. Song, Hemoglobin-imprinted polymer gel prepared using modified glucosamine as functional monomer, Chinese Chemical Letters 19 (2) (2008) 233–236.

[29] B.V.M. Silva, I.T. Cavalcanti, A.B. Mattos, P. Moura, M.D.P.T. Sotomayor, R.F. Dutra, Disposable immunosensor for human cardiac troponin T based on streptavidin-microsphere modified screen-printed electrode, Biosensors & Bioelectronics 26 (3) (2010) 1062–1067.

[30] S.K. Arya, P.R. Solanki, M. Datta, B.D. Malhotra, Recent advances in self-assembled monolayers based biomolecular electronic devices, Biosensors & Bioelectronics 24 (9) (2009) 2810–2817.

[31] B.M. Mar'yanov, E.V. Pozdnyakov, Mathematical equations for potentiometric analysis by the multiple addition method, Journal of Analytical Chemistry 61 (6) (2006) 540–543.

[32] M. Brunori, D. Bourgeois, B. Vallone, The structural dynamics of myoglobin, Journal of Structural Biology 147 (3) (2004) 223–234.

[33] M.M. Billah, C.S. Hodges, H.C.W. Hays, P.A. Millner, Directed immobilization of reduced antibody fragments onto a novel SAM on gold for myoglobin impedance immunosensing, Bioelectrochemistry 80 (1) (2010) 49–54.

[34] I.I. Suni, Impedance methods for electrochemical sensors using nanomaterials, Trac-Trends in Analytical Chemistry 27 (7) (2008) 604–611.

[35] M.A. Panagopoulou, D.V. Stergiou, I.G. Roussis, M.I. Prodromidis, Impedimetric biosensor for the assessment of the clotting activity of rennet, Analytical Chemistry 82 (20) (2010) 8629–8636.

[36] H-Y. Lin, J. Rick, T-C. Chou, Optimizing the formulation of a myoglobin molecularly imprinted thin-film polymer-formed using a micro-contact imprinting method, Biosensors & Bioelectronics 22 (12) (2007) 3293–3301.

[37] N.J. Ronkainen, H.B. Halsall, W.R. Heineman, Electrochemical biosensors, Chemical Society Reviews 39 (5) (2010) 1747–1763.

[38] S.A. Soper, K. Brown, A. Ellington, B. Frazier, G. Garcia-Manero, V. Gau, S.I. Gutman, D.F. Hayes, B. Korte, J.L. Landers, et al., Point-of-care biosensor systems for cancer diagnostics/prognostics, Biosensors & Bioelectronics 21 (10) (2006) 1932–1942.

[39] Y. Umezawa, P. Buhlmann, K. Umezawa, K. Tohda, S. Amemiya, Potentiometric selectivity coefficients of ion-selective electrodes Part I. Inorganic cations – (Technical report), Pure and Applied Chemistry 72 (10) (2000) 1851–2082.

[40] G. Horvai, The matched potential method, a generic approach to characterize the differential selectivity of chemical sensors, Sensors and Actuators B: Chemical 43 (1–3) (1997) 94–98.